J Soils Sediments (2016) 16:2306–2315
DOI 10.1007/s11368-016-1470-x

SEDIMENTS, SEC 2 • PHYSICAL AND BIOGEOCHEMICAL PROCESSES • RESEARCH ARTICLE

Effects of simulated wind followed by rain on runoff and sediment yield from a sandy loessial soil with rills

Qingyin Zhang[1] · **Jun Fan**[1,2] · **Xiaoping Zhang**[1,2]

Received: 15 September 2014 / Accepted: 3 June 2016 / Published online: 16 June 2016

Abstract
Purpose Severe soil erosion is caused by wind and water acting separately or in combination or sequentially and is an important factor affecting dryland ecosystems, especially in the severely eroded "water–wind erosion crisscross region" on the Loess Plateau. Thus, the aim of the study was to determine the magnitudes of wind and water erosion under simulative conditions and explore the mechanisms of their interactions.
Materials and methods We analyzed the interaction between these two types of erosion by exposing a sandy loessial soil with an artificial rill to simulated wind at four speeds (0, 1, 8, and 15 m s^{-1}) and then to simulated rainfall, measuring runoff, sediment yield, and characterizing changes in rill morphology. This simulated the transition period between the dry (windy) and wet seasons.
Results and discussion The time to runoff initiation depended on both wind speed and rainfall intensity, but rainfall had a larger impact on runoff. At the 15 m s^{-1} wind speed, the total runoff significantly ($P < 0.05$) increased by 33.3 kg when the rainfall intensity was increased to 120 from 60 mm h^{-1}. Under the 120 mm h^{-1} rainfall intensity, the total sediment yields increased significantly ($P < 0.05$) with increasing wind speed. Erosion sediment yields increased by 9.7, 16.3, and 70.4 % with increasing wind speed under all three rainfall intensities when compared with a no wind case. Changes in rill morphology caused by wind erosion were a factor that affected the erosion processes of subsequent rainstorms.
Conclusions Our results provide a basis for hypothesizing trends of wind and water erosion, highlight the importance of wind and water erosion acting in conjunction in semi-arid ecosystems, and are conducive for developing a more integrated perspective of wind–water dynamics on the Loess Plateau.

Keywords Sediment transport · Semi-arid region · Wind tunnel · Wind–water interaction

1 Introduction

Soil degradation and desertification lead to significant loss of soils suitable for food production. There are a number of factors that cause soil degradation and desertification including water and wind erosion, soil salinization, and soil contamination by, for example, heavy metals (Breshears et al. 2003; Ludwig et al. 2005; Amezketa 2006; Chen et al. 2015). Two of the major factors involved are water and wind erosion, which can be especially pronounced in arid and semi-arid environments where the relatively sparse vegetation cover allows wind and water energy to directly impact the soil surface to a greater degree (Breshears et al. 2003). Together, both types of erosion account for >85 % of the soil degradation in dryland areas (Middleton and Thomas 1997). Aeolian transport processes in semi-arid regions have important global implications (Cooke et al. 1993; Goudie 2008) and are perhaps most evident in major dust storms across regionally degraded landscapes (Worster 1979; Peters et al. 2007), particularly in association with the degraded drylands of northern China

Responsible editor: David Allen Lobb

✉ Jun Fan
fanjun@ms.iswc.ac.cn

[1] State Key Laboratory of Soil Erosion and Dryland Farming on the Loess Plateau, Northwest A&F University, Yangling 712100, China

[2] Institute of Soil and Water Conservation, Chinese Academy of Sciences and Ministry of Water Resources, Yangling 712100, China

(Chepil 1949; Shao and Shao 2001). The potential for soil erosion and land degradation due to the synergistic effects of wind and water erosion may far exceed that of either type alone (Bullard and Livingstone 2002). The actions of wind and water can each degrade ecosystems and accelerate desertification, and both processes acting together can contribute substantially to overall erosion (Schlesinger et al. 1990; Breshears et al. 2003; Peters et al. 2006; Okin et al. 2009).

Aeolian transport is generally recognized as important, but our current understanding and focus on aeolian processes are often in isolation from the other primary driver of land-surface dynamics: transport by water (Breshears et al. 2003; Visser et al. 2004). Research on soil erosion generally focuses on either wind or water erosion. Comparing wind and water erosion should be addressed by considering the aspects that both have in common (Toy et al. 2002). The redistribution of soil and other critical resources, such as nutrients, organic debris, seeds, and water, are driven by different physical forces, but their processes generally share three critical phases. The first phase is the detachment of soil particles from the surface by the movement of water or wind. The second phase is the transport of the detached particles as either overland flow or wind-blown suspensions. The third phase is the deposition of these particles as the wind or water speeds decline (Breshears et al. 2003). The interaction between the processes of wind and water can have a large influence on the soil in dryland environments. For example, sediments can be transported over long distances by water erosion from dry lakebeds, river beds, and floodplains and deposited as a potential future source of aeolian transportable material. Transport by wind and water can thus further redistribute the deposited sediment, therefore increasing the potential for interactions between these processes (Bullard and Livingstone 2002). Gao and Tang (1995) demonstrated in the field that sediments associated with water erosion, transport, and accumulation provided a basis for wind erosion and that material eroded by wind was, in turn, subsequently acted upon by water. Some studies have suggested that the erosive energy of wind and water combined is significantly greater than that of either alone, which could thus expand the potential area affected by erosion (Gao and Tang 1995, 1996; Gao et al. 1998).

Even though research on aeolian transport has generally been conducted in isolation from transport by water, the interrelationships between these processes should be a research priority (Heathcote 1983; Breshears et al. 2003; Bullard and Mctainsh 2003; Visser et al. 2004). An increasing number of studies (e.g., Bullard and Mctainsh 2003; Zhang et al. 2012) have demonstrated that wind and water erosion are interrelated, and that their combination exhibits clear temporal and spatial characteristics. The relationship between long-term climate change (over millennia) and wind–water activity in dryland areas has been widely recognized, as have oscillations between periods dominated by wind and water activity (Bullard and Mctainsh 2003; Clarke and Rendell 1998). The actions of wind and water can interact at global and regional scales, where aeolian landforms interact with fluvial–lacustrine systems in different climatic zones and geomorphological regions. Moreover, they can act at the scale of individual landforms where, for example, wind-created dunes are a source of material when they interact with seasonal floods (Thomas et al. 1993). Wind erosion can be increased dramatically by the abrasive action of windborne sand (Zhang et al. 2012).

Despite the importance of wind and water erosion processes in semi-arid areas and the application of conceptual models and limited field measurements in many similar environments, studies on both types of erosion in combination are scarce (Valentin 1996; Breshears et al. 2003; Visser et al. 2004). Erosion and sediment yield are particularly high in the central Yellow River basin, especially in the so-called "water–wind erosion crisscross region" on the Loess Plateau. Soil erosion and land desertification in this unique region are associated with dramatic changes of climate (Gao and Tang 1996). Erosion in the region can be as much as 10,000 t km^{-2} $year^{1}$ and may exceed this rate in some areas. Gao and Tang (1995) reported that water and wind erosion often occur alternately with the change in season in this region, which results in an unusual kind of soil erosion referred to as "complex erosion by aeolian–fluvial interaction." Furthermore, in the western part of the Liudaogou watershed, wind erosion occurs just as often as water erosion. Consequently, the rate of soil erosion is the highest occurring on the Loess Plateau and in China as a whole (Gao and Mu 2004). Episodes of natural erosion are complex and quite variable and so are difficult to study, but laboratory trials can use wind tunnels and rainfall simulators to create controlled conditions and thereby increase the amount of statistically robust data. Some laboratory facilities, such as those described by Lyles et al. (1969), de Lima et al. (1992), Gabriels et al. (1997), Fister and Schmidt (2008), and Burri et al. (2011) have the capability of simultaneously simulating rain and wind for studies of their interactions. The major advantages of rainfall and wind simulations (e.g., a high degree of repeatability and the capacity to control boundary conditions) facilitate studies of the interactions between wind and water erosion, as well as the development of a more integrated perspective of the dynamics of wind and water. An integrated perspective of the contributions of these processes to total erosion and of their variations with scale and the degree to which they interact is lacking. The major objective of this study is to explore interactions of wind and water erosion under simulative conditions.

2 Materials and methods

2.1 Equipment

The experiments were conducted in the rainfall simulator and wind tunnel laboratory of the State Key Laboratory of Soil Erosion and Dryland Farming on the Loess Plateau of the Institute of Soil and Water Conservation, Chinese Academy of Sciences and Ministry of Water Resources, in Yangling. The rainfall simulator laboratory is 48 m long by 27 m wide by 23 m high. This study simulated rainfall from lateral-jets at a height of 16 m, which projected water droplets horizontally that followed a parabolic trajectory to fall vertically and attained a terminal velocity close to that of natural rainfall over a target area of 10 m × 10 m.

The simulated rainfall intensities investigated were 60, 90, and 120 mm h^{-1}. The chosen number of nozzles and the water pressure at each nozzle, which was set so that the trajectory of the rainwater from each nozzle intersected that of the rainwater from the neighboring nozzles, ensured that the rainfall distribution was uniform over the entire surface of the soil under investigation.

The wind tunnel had a nominal cross-section of 1.2 m × 1 m and a total length of 19 m that included sections along its length for the fan (3.55 m), wind regulation (1.5 m) and rectification (10 m), test area (1.28 m), and sand collection (3.02 m). The height of the tunnel roof was adjusted for each configuration in order to ensure a pressure gradient of zero in the direction of flow and to establish a turbulent boundary layer above a fixed sub-layer in the test section (Clifton et al. 2008; Walter et al. 2009). The measuring instrumentation in the wind tunnel consisted of a traversable anemometer and a newly designed segmented sampler for wind tunnel test (Dong et al. 2004). Wind speeds could be adjusted between 0 and 15 m s^{-1}.

The wind tunnel included sand collection chambers, each 2 cm high and positioned at different heights that could facilitate the measurement of the vertical profile of the sediment-mass flux. However, in this study, the focus was only on the total amount of wind-eroded sediment material, which was collected from all of the chambers at different heights and combined. The sampler was constructed of steel (0.5 mm thick) with openings of 2 cm × 10 cm to the sand collection chambers. The sampler was placed at the far end of the test section to collect the wind-transported eroded sediment.

2.2 Experimental design and methods

The experiments consisted of four parts: collection and preparation of the soil under investigation, preparation of the pre-rill soils for the tests in a tray, and the wind and rainfall simulations. The wind and rainfall simulations were aimed at simulating the alternating cycles of winter–spring wind erosion and summer–autumn water erosion in the study region on the Loess Plateau, and specifically during the transition between those two periods.

The investigated soil was a sandy loessial soil collected from the Liudaogou watershed area in the water–wind erosion crisscross region in Shenmu County, Shaanxi Province (Fig. 1). The soil was taken from the upper 50-cm soil layer in an area without plant cover. The sandy loessial soil was air-dried and passed through an 8-mm sieve. Visible roots, stones, and other debris were removed in order to reduce variations in the erosion processes that occurred during the experiments that would be caused by their effects on clumping, roughness, and hardness. Relevant soil properties, including a detailed particle size distribution that was determined by using the pipette method (Gee and Or 2002), and classified based on the USDA system, are given in Table 1. The soil had a relatively high fine sand content (64.9 %) and low clay content (5.8 %). Hence, the soil had a loose structure with little cohesion and was highly erodible.

A tray to hold the soil was constructed of corrosion-resistant plate that was 128 cm long, 100 cm wide, and 15 cm deep. The tray was inserted into the test section of the wind tunnel. In addition, the tray was set at an adjustable slope during the rainstorms, although it was kept horizontal during the wind erosion experiments. The base of the tray had holes (5 mm in diameter at a spacing of 50 mm) to facilitate the percolation of water. In preparation for the wind and water erosion experiments, soil was packed uniformly into the trays to obtain a consistent bulk density of 1.3 g cm^{-3}, which was similar to the field bulk density. The amount of soil required was determined from the volume of the soil tray, the water content of the air-dried soil (about 2 %), and the intended bulk density (1.3 g cm^{-3}). The base of the tray was first covered with a layer of filter paper to prevent soil falling through the drainage holes. To achieve uniform packing of the tray, the soil was packed, layer by layer, to the desired bulk density in three 5-cm layers to a total depth of 15 cm. The surfaces of the lower two layers were roughened before packing the next layer in order to minimize vertical discontinuities caused by horizontal stratification.

The soil surface was sprayed evenly with 1000 ml of tap water before the rainfall simulation began in order to minimize the differences in the initial conditions. Two artificial rill channels (100 cm long, 10 cm wide, and 1.5 cm deep) were dug out along the center of the soil surface, beginning 28 cm from the upper edge, in each tray using a small shovel in order to simulate field conditions that can exist after the period of water erosion in the study region. Since the creation of such a channel in the loose dry soil would have been difficult, the addition of water also facilitated this procedure. The water was sufficient to wet the soil surface to a depth of 1.3 cm, ensuring that the sidewalls of the rill channels were initially

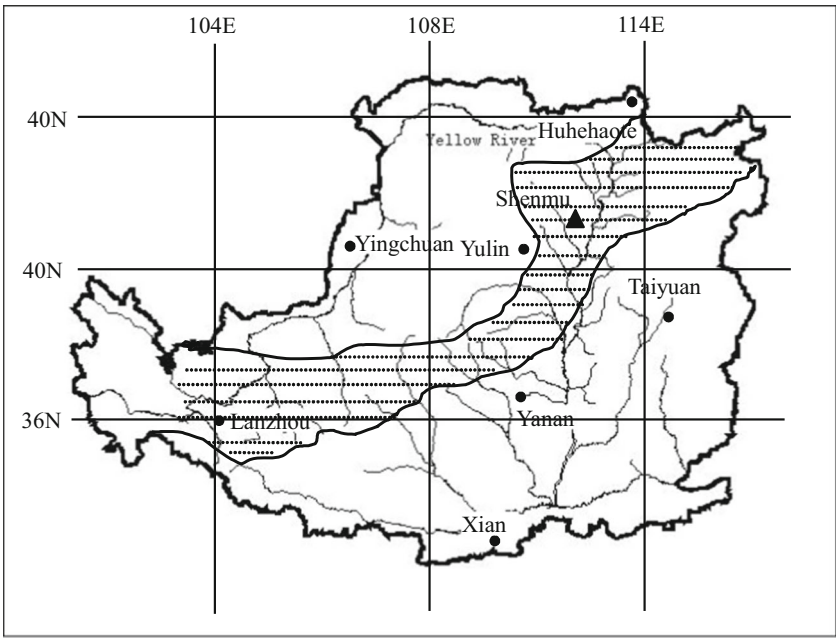

Fig. 1 The water–wind erosion crisscross region on the Loess Plateau

stable while the base of the channels were initially dry. Keeping the base of the channels dry maintained the natural loose cohesion since the addition of water would increase cohesion that would have significantly changed the susceptibility of the soil to wind erosion. Hence, the third function of adding 1000 ml of water was to confine the wind erosion to the material in the dry rill channels, and to prevent the erosion of the damp channel sidewalls and of the soil surface.

The experimental wind speeds exceeded the threshold for sediment transport, and measurements were taken only above the soil surface. Therefore, the anemometer was positioned at a height of 30 cm above the soil surface in order to measure shear stress velocity over the range of wind speeds investigated. The aeolian sediment-mass flux was measured by a newly designed segmented sampler that was constructed based on the description by Dong et al. (2004).

The wind erosion experiments were conducted first. A test soil tray was placed in the wind tunnel and exposed to wind at a designated wind speed for 10 min. Four wind speeds (0, 8, 11, and 15 m s^{-1}) were used in the study, and each treatment was tested three times. As noted above, the soil surface had been dampened for creating the rill channels such that the collected wind-borne sediment only originated from within the rills where the soil remained dry. The following formula was used to calculate the rate of wind erosion:

$$\mathrm{Re} = 6 \times We \Big/ (S \cdot T) \quad (1)$$

where Re (kg m^{-2} h^{-1}) is the rate of wind erosion (i.e., the amount of soil erosion per unit time per unit area); *We* (kg) is the amount of eroded material; *S* (m^2) is the area of soil exposed to wind erosion; *T* (h) is the exposure time; and 6 is a conversion coefficient.

The rainfall simulation experiments were conducted on the same trays following the wind simulation experiments. The rainfall intensity and effective area were calibrated before the simulated rainstorms began. The soil tray was positioned at the appropriate location under the rainfall simulator, and the slope was adjusted to 15°, which was typical of the natural slopes in the study region. Three rainfall intensities (60, 90, and 120 mm h^{-1}) were investigated. Runoff was collected at 2 min intervals following runoff initiation. The rainfall simulation continued for 40 min after runoff was initiated. The mass of the runoff with sediment that was collected during

Table 1 Key physical and chemical properties of the investigated sandy loessial soil

Clay (<0.001 mm) (%)	Fine silt (0.005–0.01 mm) (%)	Medium silt (0.01–0.05 mm) (%)	Coarse silt (0.05–0.01 mm) (%)	Fine sand (0.25–0.05 mm) (%)	Coarse sand (>0.25 mm) (%)	Bulk density (g cm^{-3})	Organic matter content (%)	Calcium carbonate content (%)
5.8	3.2	2.8	22.0	64.9	0.3	1.30	0.46	11.0

the simulated rainstorm and the mass of the sediment after oven drying at 105 °C until constant mass were determined by weighing. The amount of runoff water was determined as the mass difference before and after drying. All rainfall simulation experiments were replicated three times, to give 36 data sets.

A two-way analysis of variance (ANOVA) was used to test the effects of wind speed and rainfall intensity and their interactions on the eroded sediment yields. All statistical analyses were performed using SPSS v. 18.0 (SPSS Inc.). The significance of differences were evaluated at $P < 0.05$. Values were reported as the mean ± standard deviation, unless stated otherwise.

3 Results

3.1 Intensity of wind erosion

We ensured that the rill beds were rough to approximate natural conditions. Wind erosion rates increased exponentially and significantly ($P < 0.01$) with increasing wind speed (Fig. 2). In particular, the erosion rate was significantly and obviously higher at the wind speed of 15 m s^{-1} than at the lower speeds (Fig. 2).

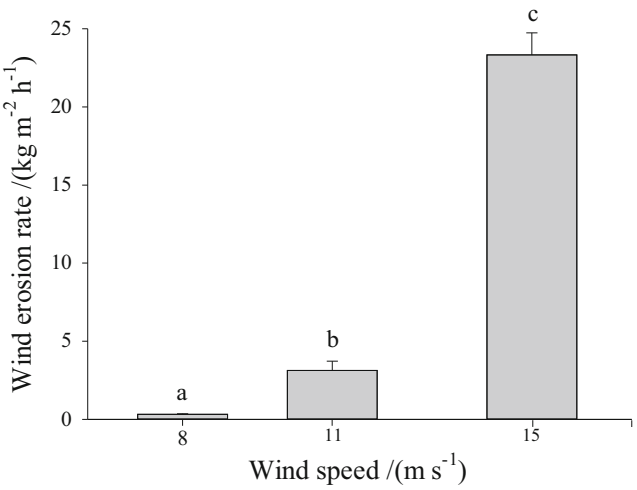

Fig. 2 Wind erosion rates at the three wind speeds. *Different letters above the bar* indicate significant differences between soil erosion rates at $P < 0.05$ (Tukey's test)

3.2 Effect of wind speed and rainfall intensity on runoff

The ANOVA results showed that both wind speed and rainfall intensity affected the time of runoff initiation (Table 2). Runoff was initiated sooner and in greater quantities as rainfall intensity increased. These results indicated that rainfall intensity was a major factor affecting runoff from slopes. Increasing the rainfall intensity led to increasing runoff production because more rainwater was supplied per unit time and the soil surface became saturated sooner; runoff rates were determined by the rainfall intensity as well as by the limitation of the soil infiltrability.

Wind speed was also an important factor affecting runoff. For example, the runoff initiation time increased by 46.1, 4.8, and 10.3 % with the increase in wind speed from 0 to 15 m s^{-1} under rainfall intensities of 60, 90, and 120 mm h^{-1}, respectively. However, the effect of wind speed was mostly not significant (Table 2), except for at a wind speed of 15 m s^{-1} under a rainfall intensity of 60 mm h^{-1}. As the wind speed increased, especially at a wind speed of 15 m s^{-1}, incidences of rill wall collapse increased, resulting in the formation of pits and dams inside the rill channels, which delayed runoff production at the beginning of the rainstorms.

The total runoff amount generally increased as wind speed increased, and this relationship became more evident as rainfall intensity increased (Fig. 3). The increase in runoff with increasing rainfall duration was similar for the three rainfall intensities. The amount of runoff was relatively small when the rainstorm began because the soil was dry and the potential for infiltration was high. Runoff then increased rapidly as the rainfall duration increased because: (1) as the soil became more saturated, the effect of matric suction at the wetting front was reduced and infiltration declined; and (2) in addition, a surface seal may have been formed that would further reduce infiltration. In all cases, the runoff increased more rapidly after 25 to 30 min of rainfall, which represented an inflexion point. This was due to the changes in the relative importance of runoff and infiltration, as well as to rill formation, as the rainstorm progressed. Greater runoff amounts occurred under the higher rainfall intensities. For example, when the wind speed was 15 m s^{-1}, the total runoff amount was 33.3 kg greater under a rainfall intensity of 120 mm h^{-1} than under 60 mm h^{-1}. However, under a fixed rainfall intensity (60, 90, and 120 mm h^{-1}), there were no significant differences ($P > 0.05$) in total runoff values among the wind speeds. The mean runoff (24.3 ± 0.4 kg) of the four wind treatments under a rainfall intensity of 60 mm h^{-1} was nearly one third of that under an intensity of 120 mm h^{-1} (61.8 ± 4.6 kg), and was lower than under 90 mm h^{-1} (35.8 ± 1.6 kg).

3.3 Effect of wind speed and rainfall intensity on sediment yield

Runoff was typically accompanied by the transport of sediment, and the sediment yield was affected by rainfall intensity and by rainfall duration (Fig. 4). The changes in sediment yields with rainfall duration under all the rainfall intensities was characterized by small initial changes followed by more rapid increases about 30 min after runoff was initiated. The changes in sediment yield indicated that different processes were associated with the production of sediment. In the first

Table 2 Effect of rainfall intensity (RI) and wind speed (WS) on runoff production

RI	60					90					120				
WS	0	8	11	15		0	8	11	15		0	8	11	15	
TRI	18.0 ± 1.2Aa	18.5 ± 1.4Aa	19.3 ± 1.5Aa	26.3 ± 2.8Ba		10.5 ± 2.0Ab	10.5 ± 0.8Ab	10.5 ± 1.9Ab	11.0 ± 2.3Ab		7.1 ± 1.6Ac	7.0 ± 1.3Ac	7.3 ± 0.9Ac	7.8 ± 1.2Ac	

TRI values followed by the same uppercase or lowercase letter did not differ significantly for different wind speeds under the same rainfall intensity or for different rainfall intensities under the same wind speed, respectively ($P < 0.05$) (Tukey's test at $\alpha = 0.05$)

RI rainfall intensity (mm h^{-1}), *WS* wind speed (m s^{-1}), *TRI* time to runoff initiation (min)

25 to 30 min, the relatively small increases in sediment yield (Fig. 4) were associated with steadily increasing runoff amounts as rainfall duration increased (Fig. 3). Runoff rates had noticeably increased after about 25 to 30 min (Fig. 3), while sediment yield increased more rapidly after about 30 min (Fig. 4). Therefore, the more rapid increases in sediment yields were likely due to the increased amounts of runoff and an associated onset or accelerated development of rill formation. Increasing the rainfall intensity increased erosion throughout a rainstorm and especially increased rill erosion during the latter part of the rainstorm. For example, when the preceding wind speed was 15 m s^{-1}, the total sediment yield was 4.1 kg greater under the subsequent rainfall intensity of 120 mm h^{-1} than under 60 mm h^{-1}.

The wind speed used to erode the soil in the rill channels prior to the rainstorms also affected water erosion such that sediment yield generally increased with the increase in wind speed under all rainfall intensities (Fig. 4). The effect of wind erosion on sediment yield was most pronounced for soil that had been initially subjected to the highest wind speed (15 m s^{-1}). Under the simulated rainfall, this soil initially had the lowest sediment yields, which was especially clear in the case of the 120 mm h^{-1} rainfall intensity, but after about 30 min of runoff, the sediment yields were the highest. Increases in total sediment yield were significant ($P < 0.05$) as rainfall intensity increased for the soils subjected to the 15 m s^{-1} wind speed with the incremental rainfall intensity. Under the 120 mm h^{-1} rainfall intensity, the total sediment yields increased significantly with increases in wind speed ($P < 0.05$); the total sediment yields from soils subjected to a wind speed of 15 m s^{-1} were 2.8 kg greater than those from soils that were not exposed to wind. Furthermore, as compared with the soil that was not exposed to wind, the water-eroded sediment yields increased by 9.7, 16.3, and 70.4 % with increasing wind speed under rainfall intensities of 60, 90, and 120 mm h^{-1}, respectively.

4 Discussion

4.1 Intensity of wind erosion

The wind tunnel facility did not allow climate control, so air temperature and humidity varied slightly during the experimental study period as actual weather conditions changed outside of the laboratory. The extent to which these slight fluctuations affected the results could not be determined without further extensive experimentation under different conditions, which was beyond the scope of this study. However, air humidity has been reported to affect the threshold shear stress for the entrainment of sediments from certain soil types during wind erosion (Neuman 2003; Cornelis et al. 2004; Ravi et al. 2006). Even so, because the soil used in this study had a coarse

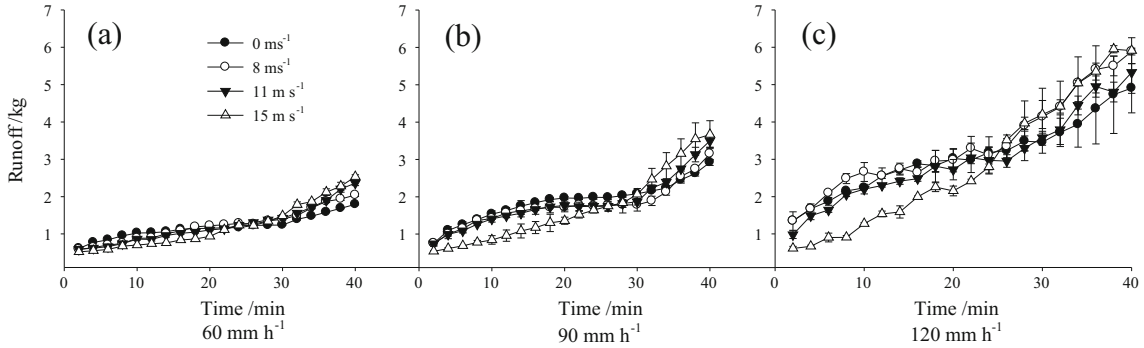

Fig. 3 Runoff over time following runoff initiation from soils exposed to various wind speeds prior to rainfall at intensities of **a** 60, **b** 90, and **c** 120 mm h^{-1}

sandy texture with a large fine sand component and exhibited weak cohesion, the applied wind speeds were above the threshold for particle entrainment. Therefore, it was reasonable to assume that any differences in air temperature and/or humidity had only minor effects on the amount of wind erosion (Burri et al. 2011).

The erosion rate was significantly higher at the wind speed of 15 m s^{-1} than at the lower speeds. This was mainly because grains of sand exposed to stronger winds with higher wind speeds were more readily dislodged from the bed of the rill channel in greater quantities, and were more readily transported suspended in the faster airflows. The sand grains moved at speeds determined by the wind speed of the airflow and gained momentum. Sand blowing within the rill channels could retain considerable momentum due to limited air resistance (Yao et al. 2004). Sand grains colliding with the sidewalls and beds of the rill channels could dislodge other grains as part of a saltation process, thereby further increasing the erosion to levels above that caused by the wind alone (Zhou et al. 1994). Notably, wind erosion rates (0.12 kg m^{-2}) were less in the study of Farsang et al. (2012, 2013) than in ours for the same wind speed and time. The increased development of rill channels could explain this phenomenon. In our study, sand grains from the walls created pits and mounds within the rill channel which occurred slightly under the 8 and 11 m s^{-1} wind speed treatments. At the 15 m s^{-1} speed, however, the severity of the wind erosion, which was enhanced by the abrasive action of wind-borne sand particles, caused rill channel walls to collapse. Furthermore, additional rill wall collapses and headward erosion expanded the rill area and increased wind erosion.

4.2 Effects of wind speed and rainfall intensity on the morphology of rills

Liu and Coulthard (2015) reported that aeolian- and fluvial-induced changes to landscape morphology were clearly widespread in the study region. Our results indicate visible changes of rill morphology after the erosion processes that occurred under wind and water erosion. These processes included headward erosion, rill incision, and rill wall collapse that occurred within the rill and affected its development. These processes and their interactions caused the rills to lengthen, deepen, and widen (Han et al. 2002). Sediment yields associated with wind and water erosion in some soil structures and surface morphologies should develop steadily before rills begin to develop, but the formation of a rill affects sediment yield

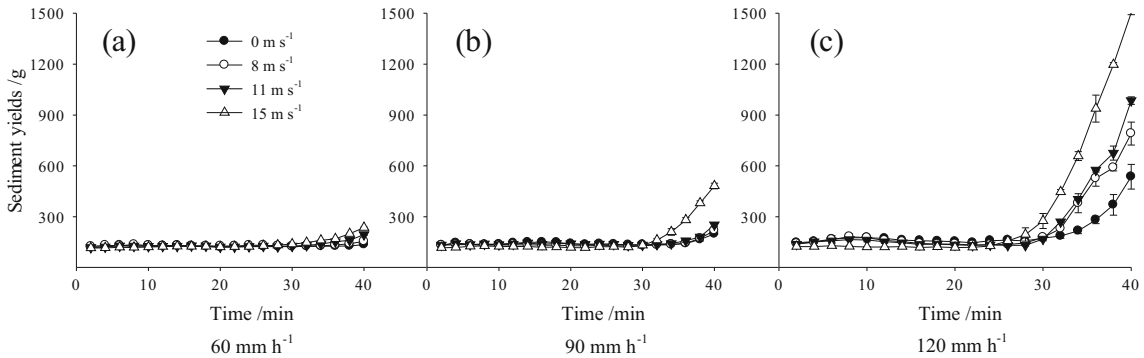

Fig. 4 Sediment yield over time following runoff initiation from soils exposed to various wind speeds prior to rainfall at intensities of **a** 60, **b** 90, and **c** 120 mm h^{-1}

depending on its morphology (Han et al. 2003). Changes in rill morphology at a wind speed of 15 m s^{-1} and under a rainfall intensity of 120 mm h^{-1} are shown in Fig. 5.

Under this treatment combination, severe rill wall collapse and gravitational erosion occurred, leading to increases in the mean rill depth and rill width of 5.8 and 3.5 cm, respectively. Little headway erosion took place in the case of wind erosion. However, the loose soil particles from the easily disintegrated aggregates that lacked strong cohesion were readily transported by wind, but were also deposited and accumulated along the rill bed. Therefore, the effects of wind erosion on rill morphology were mainly characterized by rill wall collapse and particle accumulation at the end of the rill channel. Zhou et al. (1994) reported that the intensity of wind erosion could be greatly increased if moving grains struck the soil surface and dislodged other grains, thus creating a stronger destructive force that could affect soil surface structure. Our study also demonstrated that the walls and upper sections of the rill channel were readily eroded by wind, and that the abrasive action of wind-blown sand was likely an active agent affecting rill morphology. In turn, the width, density, and depth of rill channels would be key factors that affected the amount of sediment produced by wind erosion (Zhang et al. 2012).

Loose soil particles, resulting from the destruction of the aggregates exposed to the abrasive wind erosion forces, were present on the rill beds and had accumulated at the ends of the rill channels (Fig. 5a). These loose particles provided the main initial source of transportable material for subsequent water erosion once runoff commenced and water flowed in the rills. Midway through the simulated rainstorm, the action of rill flow had caused slumping and further erosion of the rill banks exploiting the erosion damage caused by the wind; some deposition on the rill bed was also evident (Fig. 5b). Later in the rainstorm, multiple feeder rills that could channel additional runoff water and sediment into the main rill were apparent; these features had possibly been initiated by the wind erosion and developed further under water erosion. A further feature of the change in rill morphology by the highest wind speed was the formation of pits and mounds along the rill channel due to rill wall collapse. Initially, such features impeded the flow of water causing sediment deposition. The presence of the mounds may even have forced water flowing in the rills to erode the channel walls to a greater extent, thereby widening the rills. Widening the rills could decrease flow velocities that would lead to larger areas of deposition of sediments as shown in Fig. 5c. However, overall erosion increased as the rainstorms continued.

Sankey and Draut (2014) found that aeolian sediment transport processes could enhance or impede the expansion of gullies. In contrast, El-Baz et al. (2000)) illustrated that the sand of the Sahara mainly originated from fluvial processes, and was deposited in inland lacustrine depressions by palaeo-rivers and streams. In this study, the total eroded sediment yields increased by 9.7, 16.3, and 70.4 % within rainfall intensity treatments of 60, 90, and 120 mm h^{-1}, respectively, as compared with the zero wind speed treatment. Fluvial erosion and transport can concentrate or expose new sediment, increasing availability for subsequent aeolian transport (Field et al. 2009).

4.3 Applications and implications

Our results may be applicable to other semi-arid ecosystems. However, many factors can vary among ecosystems. The limitations of our simulations prevent broad inferences across different types of ecosystems; however, the trends may be suitable for the water–wind erosion crisscross region on the Loess Plateau as well as similar regions.

One of the strong features of our study was the ability to pair measurements and extrapolations of wind and water erosion under conditions simulating those of a semi-arid region. The magnitudes of wind and water erosion and of sediment transport can potentially be influenced by several factors existing in both laboratory simulations and field studies, such as some climatic drivers (e.g., distributions of rainfall and wind speed), surface characteristics (e.g., depth and width of rills), and soil properties (e.g., soil-moisture distributions and, especially, soil textures) (Breshears et al. 2003). To ensure the success of our simulations, artificial rill channels were formed,

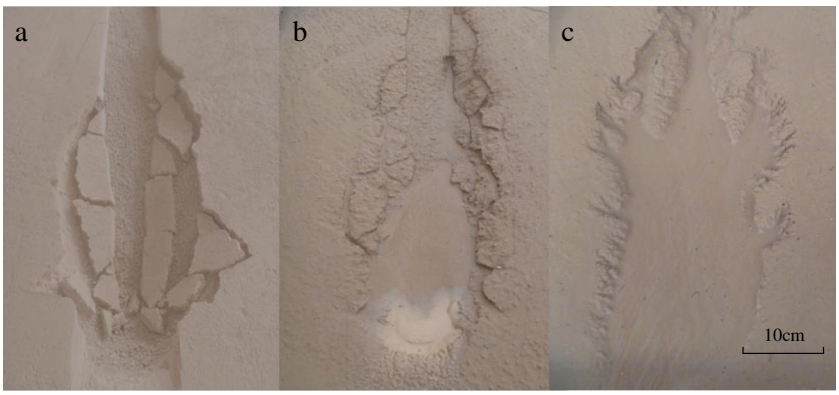

Fig. 5 Changes in rill morphology due to wind (15 m s^{-1}) and water (120 mm h^{-1}) erosion. The flow direction was from *top* to *bottom*. **a** After the wind erosion but before the rainfall, **b** midway during the rainstorm, and **c** towards the latter stage of the rainstorm

and the soil surfaces were wetted before the simulations began. We conducted wind erosion simulations after forming the artificial rill channels instead of using rill channels created by simulated rainfall because a long time may be required before the rills are formed by water erosion. Furthermore, at the low wind speeds produced by the small wind tunnel, differences in wind erosion effects might not be distinct due to crust formation after or during water erosion. Therefore, these experimental conditions simulated those during the transition from the dry wind erosion season to the wet water erosion season on the Loess Plateau. However, the small size of the soil tray limited our ability to simulate erosion from upslope runoff, which would occur under natural conditions. Field monitoring is thus needed to determine better the larger-scale transport of sediments.

5 Conclusions

This study examined the effects of simulated wind and water erosion of a sandy loessial soil during the transition period from the dry to wet seasons in a semi-arid region. Runoff and sediment yield of the sandy loess increased with rainfall duration after runoff initiation, and these changes were significantly correlated with the rate of wind erosion (a function of wind speed) and rainfall intensity. The time to runoff initiation was influenced more by rain intensity than by wind speed and increased by 46.1, 4.8, and 10 3 % with the overall increase in wind speed (from 0 to 15 m s^{-1}) at rainfall intensities of 60, 90, and 120 mm h^{-1}, respectively.

Runoff and sediment yield during the first 25 min of runoff production were lower for soils that had been exposed to a wind speed of 15 m s^{-1} than to one of 8 m s^{-1}; however, this trend was reversed after 30 min of runoff. For soil exposed to 15 m s^{-1} wind speed, the total runoff under a rainfall intensity of 120 mm h^{-1} increased by 33.3 kg over that produced by the 60 mm h^{-1} rainstorm. However, under a rainfall intensity of 60 mm h^{-1}, there were no significant differences ($P > 0.05$) in total runoff amounts among the different wind speeds. Under the 120 mm h^{-1} rainfall intensity, the total sediment yields increased significantly with the increasing wind speed ($P < 0.05$). Similarly, under the 15 m s^{-1} wind speed treatment, yields increased significantly with increases in rainfall intensity. The total eroded sediment yields increased by 9.7, 16.3, and 70.4 % with increasing wind speed above 0 m s^{-1} for rainfall intensities of 60, 90, and 120 mm h^{-1}, respectively.

Wind erosion, along with the abrading action of windborne sand grains, altered rill morphology and disintegrated soil aggregates, thereby providing loose micro-aggregates and soil particles to be further transported by water during the subsequent rainstorm. The rills that developed under the rainfall further altered the soil surface that might then lead to enhanced wind erosion, although this was not measured in this study. Rain and wind could thus interact synergistically to increase erosion, each possibly increasing the effect of the other when they occur sequentially.

Acknowledgments We acknowledge funding by The National Natural Science Foundation of China (Nos. 41571130082, 51239009, 41271239). We are grateful to the three anonymous reviewers for their helpful suggestions.

References

Amezketa E (2006) An integrated methodology for assessing soil salinization, a pre-condition for land desertification. J Arid Environ 67: 594–606

Breshears DD, Whicker JJ, Johansen MP, Pinder JE (2003) Wind and water erosion and transport in semi-arid shrubland, grassland and forest ecosystems: quantifying dominance of horizontal wind-drive transport. Earth Surf Process Landforms 28:1189–1209

Bullard JE, Livingstone I (2002) Interactions between aeolian and fluvial systems in dryland environments. Area 34:8–16

Bullard JE, McTainsh GH (2003) Aeolian-fluvial interactions in dryland environments: examples, concepts and Australia case study. Prog Phys Geog 27:47l–501

Burri K, Gromke C, Lehning M, Graf F (2011) Aeolian sediment transport over vegetation canopies: a wind tunnel study with live plants. Aeolian Res 3:205–213

Chen HY, Teng YG, Lu SJ, Wang YY, Wang JS (2015) Contamination features and health risk of soil heavy metals in China. Sci Total Environ 512:143–153

Chepil WS (1949) Wind erosion control with shelterbelts in North China. Agron J 41:127–129

Clarke ML, Rendell HM (1998) Climate change impacts on sand supply and the formation of desert sand dunes in the southwest USA. J Arid Environ 39:517–531

Clifton A, Manes C, Rueedi JD, Guala M, Lehning M (2008) On shear-driven ventilation of snow. Bound-Lay Meteorol 126:249–261

Cooke RU, Warren A, Goudie AS (1993) Desert geomorphology. UCL Press, London, UK

Cornelis WM, Oltenfreiter G, Gabriels D, Hartmann R (2004) Splash-saltation of sand due to wind-driven rain: vertical deposition flux and sediment transport rate. Soil Sci Soc Am J 68:32–40

De Lima JL, van Dijk PM, Spaan WP (1992) Splash-saltation transport under wind-driven rain. Soil Technol 5:151–166

Dong ZB, Sun HY, Zhao AG (2004) WITSEG sampler: a segmented sand sampler for wind tunnel test. Geomorphology 59:119–129

El-Baz F, Maingue M, Robinson C (2000) Fluvio-aeolian dynamics in the north-eastern Sahara: the relationship between fluvial-aeolian systems and ground-water concentration. J Arid Environ 44:173–183

Farsang A, Gergely Kitka KB, Puskas I (2012) Estimating element transport rates on sloping agricultural land at catchment scale. Carpathian J Earth Environ Sci 7:15–26

Farsang A, Duttmann R, Bartus M, Szatmari J, Barta K, Bozso G (2013) Estimation of soil material transportation by wind based on in situ wind tunnel experiments. J Environ Geogr 6:13–20

Field JP, Breshears DD, Whicker JJ (2009) Toward a more holistic perspective of soil erosion: why aeolian research needs to explicitly consider fluvial processes and interactions. Aeolian Res 1:9–17

Fister W, Schmidt RG (2008) Concept of a single device for simultaneous simulation of wind and water erosion in the field. In: Combating desertification: assessment, adaptation and mitigation strategies:

Proceedings of the Conference on Desertification, 23.01.2008, Ghent, Belgium, pp. 106-113
Gabriels D, Cornelis WM, Pollet I, van Coillie T, Ouessar M (1997) The ICE wind tunnel for wind and water erosion studies. Soil Technol 10:1–8
Gao ZL, Mu XM (2004) Spatio-temporal change of land use/coverage in loess wind-water erosion crisscross region. J Soil and Water Conserv 18:146–150
Gao XT, Tang KL (1995) Erosion strains and characteristics of wind and water erosion interaction I Shenfu-Dongsheng coal mining area. Bull Soil Water Conserv 15:33–38
Gao XT, Tang KL (1996) Study on erosion energy of wind-water erosion. Bull Soil Water Conserv 16:27–31
Gao XT, Hou QC, Tang KL (1998) A study on characteristics of wind-water erosion interaction in Shujigou watershed, Shenfu Coal Mining area, Shannxi Province. Arid Land Geog 21:34–39
Gee GW, Or D (2002) Particle-size analysis. In: Dane JH, Topp GC (Eds.), Methods of soil analysis. Part 4. Physical methods. Soil Science Society of America Book Series No. 5, pp. 255-289
Goudie AS (2008) The history and nature of wind erosion in deserts. Annu Rev Earth Planet Sci 36:97–119
Han P, Ni JR, Li TH (2002) Headcut and bank landslip in rill evolution. J Basic Sci Eng 10:115–125
Han P, Ni JR, Wang XK (2003) Experimental study on gravitational erosion process. J Hydraul Eng-ASCE 1:51–57
Heathcote RL (1983) The arid lands: their use and abuse. Longman, New York, USA
Liu BL, Coulthard TJ (2015) Mapping the interactions between rivers and sand dunes: implications for fluvial and aeolian geomorphology. Geomorphol 231:246–257
Ludwig JA, Wilcox BP, Breshears DD, Tongway DJ, Imeson AC (2005) Vegetation patches and runoff-erosion as interacting ecohydrological processes in semiarid landscapes. Ecology 86:288–297
Lyles L, Disrud LA, Woodruff NP (1969) Effects of soil physical properties, rainfall characteristics, and wind velocity on clod disintegration by simulated rainfall. Soil Sci Soc Am Proc 33:302–306
Middleton N, Thomas D (1997) World atlas of desertification, 2nd edn. Arnold, London, UK
Neuman CM (2003) Effects of temperature and humidity upon the entrainment of sedimentary particles by wind. Bound-Lay Meteorol 108:61–89
Okin GS, Parsons AJ, Wainwright J, Herrick JE, Bestelmeyer BT, Peters DPC, Fredrickson EL (2009) Do changes in connectivity explain desertification? BioScience 59:237–244
Peters DPC, Bestelmeyer BT, Herrick JE (2006) Disentangling complex landscapes: new insights into arid and semiarid system dynamics. BioScience 56:491–501
Peters DPC, Sala OE, Allen CD, Covich A, Brunson M (2007) Cascading events in linked ecological and socio-economic systems: predicting change in an uncertain world. Front Ecol Environ 5:221–224
Ravi S, Zobeck TM, Over TM, Okin GS, D'Odorico P (2006) On the effect of moisture bonding forces in air-dry soils on threshold friction velocity of wind erosion. Sedimentol 53:597–609
Sankey JB, Draut AE (2014) Gully annealing by aeolian sediment: field and remote-sensing investigation of aeolian–hillslope–fluvial interactions, Colorado River corridor, Arizona, USA. Geomorphol 220: 68–80
Schlesinger WH, Reynolds JF, Cunningham GL, Huenneke LF, Jarrell WM, Virginia RA, Whitford WG (1990) Biological feedbacks in global desertification. Science 247:1043–1048
Shao YP, Shao SX (2001) Wind erosion and wind erosion research in China: a review. Ann Arid Zone 40:317–336
Thomas DSG, Nash DJ, Shaw PA (1993) Present day lunette sediment cycling at Witpan in the arid southwestern Kalahari Desert. Catena 20:515–527
Toy TJ, Foster GR, Renard KG (2002) Soil erosion: processes, prediction, measurement, and control. John Wiley & Sons, New York, USA
Valentin C (1996) Soil erosion under global change. In: Walker B, Steffen W (eds) Global change and terrestrial ecosystems. Cambridge University Press, New York, USA, pp 317–338
Visser SM, Sterk G, Ribolzi O (2004) Techniques for simultaneous quantification of wind and water erosion in semi-arid regions. J Arid Environ 59:699–717
Walter B, Gromke C, Lehning M (2009) The SLF boundary-layer wind tunnel—an experimental facility for aerodynamical investigations on living plants. Proceedings of the 2nd International Conference on Wind Effects on Trees, University of Freiburg, Germany, October 13–16, 2009
Worster D (1979) Dust bowl: the Southern Plains in the 1930s. Oxford University Press, New York, USA
Yao WM, Yun LY, Feng HM (2004) Wind drift and kinematics. Distant Publishing House, China, pp 94–99
Zhang QY, Fan J, Zhang XP (2012) Effects of water erosion on wind erosion in wind tunnel. J Soil Water Conserv 26:75–79
Zhou XY, Liu YZ, Wu D (1994) A study on some special ground wind erosion in the tunnel. Geogr Res 13:41–48